

## Granite fabrics and regional-scale strain partitioning in the Seridó belt (Borborema Province, NE Brazil)

Carlos J. Archanjo,<sup>1</sup> Ricardo I. F. Trindade,<sup>2</sup> Jean Luc Bouchez,<sup>3</sup> and Marcia Ernesto<sup>2</sup>

Received 7 November 2000; revised 8 August 2001; accepted 12 September 2001; published 26 January 2002.

[1] Fabrics of the Brasiliano-age granitoid plutons of the Seridó belt (northeastern Brazil) were organized following the partitioned regional strain field which shaped larger areas of the basement and its metapelitic cover. Nine plutons located at the central and western portions of the belt have been investigated by means of anisotropy of magnetic susceptibility. These plutons, emplaced between 580 and 575 Ma, are mainly potassic calc-alkalic magnetite-bearing monzogranites. The presence of primary coarse-grained magnetite as the main magnetic mineral is indicated by optical and electronic microscopy, magnetic susceptibilities, hysteresis ratios, and thermomagnetic curves. The plutons show a strong internal coherence of magnetic fabric, with foliation poles distributed around a zone axis parallel to the gently plunging mean lineation. The magnetic fabric was used to trace the strain partitioning along the belt. In the central transpressive shear belt the magnetic lineations are parallel to north trending regional stretching. On the other hand, in the western basement block a voluminous granitic magmatism was emplaced as a consequence of a transtensional/extensional deformation. Lineations in these granites trend in a NE direction, which is parallel to the transport, inferred from kinematic indicators along the shear zones. A crustal-scale east trending dextral shear zone connects both the transtensional and transpressional domains. **INDEX TERMS:** 1518 Geomagnetism and Paleomagnetism: Magnetic fabrics and anisotropy; 8035 Structural Geology: Pluton emplacement; 8110 Tectonophysics: Continental tectonics—general (0905); 9619 Information Related to Geologic Time: Precambrian; **KEYWORDS:** Anisotropy of magnetic susceptibility (AMS), granite, strain partitioning, NE Brazil

### 1. Introduction

[2] Fabrics in granitic magmas may form in response to a variety of processes, including body forces due to magma chamber dynamics and surface forces related to the imposed regional tectonic strain onto the magma body. The degree of structural continuity between magmatic and host rock fabrics has been used to infer the degree of mechanical coupling between magma dynamics and regional strain [see *Paterson et al.*, 1998]. Magmatic fabrics formed by body forces should not be mechanically coupled to the host rock structure. In contrast, continuity of magmatic structures with synemplacement

host rock structures should indicate a mechanical coupling between pluton and host rocks that may typify syntectonic intrusions [*Hutton*, 1988]. This relatively simple picture may be useful if the strain field of the whole system is homogeneous. However, the high contrast of viscosity resulting from the presence of melt in a deforming crust implies that the strain must be heterogeneous on various scales [*Vigneresse and Tikoff*, 1999]. Because of their contrasting rheologies the deformation of the magma and the solid phases may become decoupled, which results in strain partitioning. The melt preferentially accommodates the noncoaxial deformation which enhances the asymmetry of the fabric. The resulting strain pattern can be variable within a single pluton or from one pluton to another despite emplacement in a specific tectonic setting [*Gleizes et al.*, 1997].

[3] The depth of emplacement is another critical factor in determining the degree of fabric continuity in syntectonic plutons [*Schofield and D'Lemos*, 1998]. Fabrics due to melt ascent should be preserved in granitoids intruding the upper crust because faster cooling rates should prevent the crystallizing magma from undergoing significant tectonic strain. At increasing intrusion depths, development of tectonic-related magmatic fabrics is expected because slower cooling rates favor longer time for pluton crystallization to be completed. In this way, it has been suggested that deep-seated plutons with a remarkable homogeneity of fabric in continuity to the host rock structures can be used as markers of the regional strain regime [*Archanjo et al.*, 1992; *Gleizes et al.*, 1997; *Paterson et al.*, 1998]. Postemplacement processes, such as the extrusion of a partially molten body by tectonic shortening [*Davidson et al.*, 1996] or sinking of the pluton floor due to replenishment of the chamber by mafic (dense) magmas [*Wiebe and Collins*, 1998], may complicate such scenarios.

[4] In the Seridó belt (SeB, northeast Brazil; Figure 1), granite plutons were emplaced in a ductile and extensively migmatized crust during the Brasiliano/Pan-African orogeny. This belt, more than 45,000 km<sup>2</sup>, has a special geodynamic significance in the assembly of the West Gondwana since situated at intersection of EW trending lineaments more than 1000 km long that merge in NE trending lineaments that run ~3000 km from central Brazil to Nigeria and Hoggar Shields in Africa. Numerical modeling simulating the movement of this fault system predicts significant perturbations of the finite strain field, as localization of deformation along branched shear zones, lateral variations in strain intensity, and deformations regimes [*Tommasi and Vauchez*, 1997]. Many granitic plutons intrude near or along shear zones, suggesting that magmatism and deformation are related features. These relationships were investigated in nine plutons using anisotropy of magnetic susceptibility (AMS) measurements. The theoretical background of the AMS is described elsewhere [*Borradaile and Henry*, 1997; *Bouchez*, 1997], the essence being that AMS provides a fast determination of igneous fabric on granitoids that appear massive in the field. In this paper we present the main

<sup>1</sup>Instituto de Geociências, Universidade de São Paulo, São Paulo, Brazil.

<sup>2</sup>Instituto Astronômico e Geofísico, Universidade de São Paulo, São Paulo, Brazil.

<sup>3</sup>Equipe de Pétrophysique, Université Paul-Sabatier, Toulouse, France.

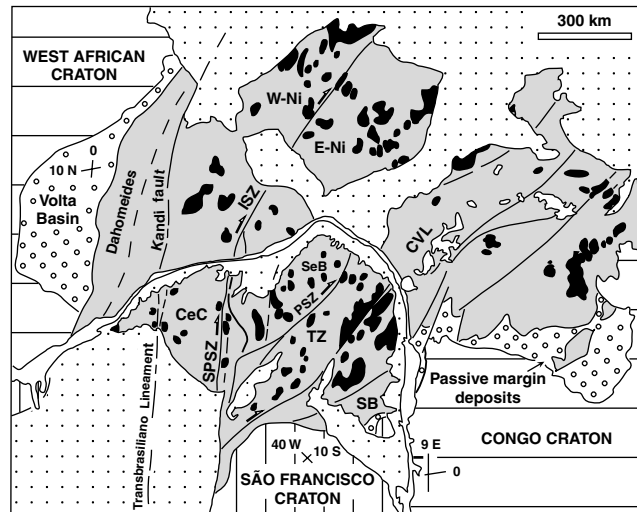


**Figure 1.** Pre-Mesozoic fit between Borborema Province in northeast Brazil and Nigeria and Cameroon shields (shaded areas) in Africa, showing the main granitic rocks (solid) and shear zones (modified from *Unrug [1996]*). W-Ni and E-Ni, western and eastern Nigerian basement; CVL, Cameroon volcanic line of Tertiary age. Borborema Province: CeC, Ceará Central; SeB, Seridó belt; TZ, Transversal Zone; SB, Sergipano belt. SPSZ, ISZ and PSZ are the shear zones of Senador Pompeu, Ile-Ife, and Patos, respectively.

structural features of the Seridó domain and enclosed plutons, as well as a detailed description of two key areas: the Acari-Totoró and the Prado-Caraúbas magmatic complexes. We discuss the significance of their magnetic fabrics and present a regional tectonic model that incorporates these data.

## 2. Geological Setting

[5] The Borborema Province (NE Brazil) is crosscut by a set of continental-scale shear zones [*Vaucher et al., 1995*] that juxtapose terranes with different evolutions. In a pre-Mesozoic configuration (Figure 1), these shear zones run from Brazil to Hoggar through the Igara/Jos-Adamawa basement of eastern Nigeria [*Black et al., 1994; Caby, 1989; Ferré et al., 1995*]. In the eastern Borborema Province, the east trending Patos shear zone (PSZ; Figure 1) separates a northern block of Paleoproterozoic to Archean rocks that form the basement of the Seridó schist belt, from a southern block comprising the Meso- to Neoproterozoic rocks of the Transversal Zone [*Brito Neves et al., 1995; Van Schmus et al., 1995*].

### 2.1. Seridó Domain

[6] The Seridó belt (SeB) comprises the central NE trending schist belt (Figure 2), and is flanked to the west by the Rio Piranhas block (RPB), and to the east by the São José de Campestre block (SJC). The SeB encloses Neoproterozoic medium- to low-grade schists and minor amounts of quartzite and conglomerate. A platform-like carbonate-quartzite association (Jucurutu rocks; not represented in Figure 2) may occur at the base of metapelites or as elongated synformal keels in the basement. The Rio Piranhas block is mainly composed of fine- to medium-grained gray gneisses intruded by augen-gneisses. It consists mostly of Trans-Amazonian rocks (2.0 to 2.2 Ga) severely deformed and migmatized during the Brasiliano orogeny [*Souza et al., 1993; Van Schmus et al., 1995*].

The São José de Campestre block is characterized by a Archean nucleus 3.45 Ga to 3.2 Ga in age [*Dantas et al., 1998*] surrounded by Paleoproterozoic rocks similar in age and composition to the units found in the western block.

### 2.2. Structural Pattern in the Schist Belt

[7] The Brasiliano deformation in the metapelitic units is characterized by a main phase that formed upright to inclined, open to tight NE trending folds, associated with a variably dipping foliation with a common fanlike appearance. In the cores of large synclinal structures, greenschist facies conditions are preserved. The metapelites frequently display a spaced cleavage defined by millimeter-scale biotite segregations which did not erase the sedimentary bedding [*Caby et al., 1995*]. Approaching the NE trending transcurrent shear zones, the metamorphic foliation grades into a typical mylonitic foliation that developed under amphibolite facies conditions. Folded and stretched aplitic to quartz-rich veins deformed in the mylonitic foliation indicated a strong component of flattening nearly perpendicular to the belt [*Archanjo and Bouchez, 1991*]. Generally the mylonitic foliation progressively decreases in dip toward low-angle shear zones. Such a low-angle fabric locally characterizes frontal ramps where slices of basement rocks are thrust upon the Seridó schist, as in the north of the Acari pluton (Figures 3 and 10). Small to moderate obliquities between the stretching directions of the low-angle fabrics ( $L_2$ ) and the superimposed vertical fabric ( $L_3$ ) may be observed in the basement as well as in the metapelitic cover. For example, between Lajes and São Tomé the mean lineation obliquity between the low-angle and vertical domains is  $8^\circ$ , whereas more westward around the São Rafael pluton, the mean obliquity reaches  $35^\circ$  (Figure 4). The north to NNW trends of the low-angle fabric occupy large areas of the basement, as in around the Picuí pluton and around Caicó (Figure 3), where the

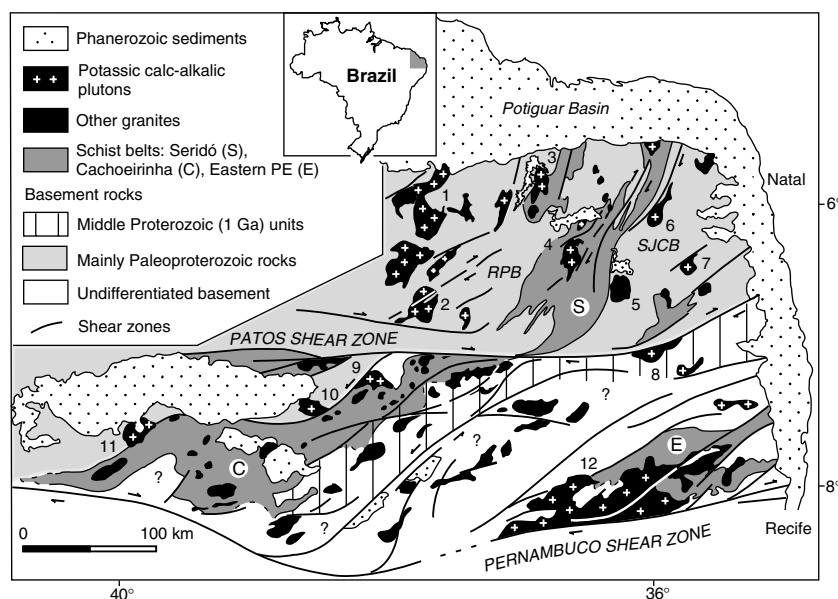


**Figure 2.** Borborema Province highlighting the distribution of the main Brasiliano plutonic rocks and shear zones. Porphyritic K-calc alkaline plutons: 1, Caraúbas-Tourão; 2, Pombal; 3, São Rafael; 4, Acari; 5, Picuí; 6, Barcelona; 7, Monte das Gameleiras; 8, Esperança; 9, Itaporanga; 10, Serra da Lagoinha; 11, Bodocó; 12, Caruaru-Serra da Japicanga. RPB and SJC are the Rio Piranhas and São José de Campestre blocks, respectively.

obliquity with the steep, NE to NNE trending lineations in the shear zones locally reaches  $60^\circ$ . Such a complex structural pattern gives rise to several geodynamic interpretations. The two fabrics were ascribed either to a polyphase deformation within the Brasiliano orogeny [Archanjo and Bouchez, 1991; Cabby *et al.*, 1995; Hackspacher *et al.*, 1997] or to a polyorogenic evolution [Jardim de Sá *et al.*, 1995] in which the low-angle fabric is considered to be much older (Paleoproterozoic) than the transpressive shear zones of Brasiliano age.

### 2.3. Structural Pattern in the Rio Piranhas Block

[8] Recent studies in the western part of the Rio Piranhas block have shown a rather different deformation pattern from that found in the Seridó schist belt [Archanjo *et al.*, 1998; Trindade, 1999]. In the Rio Piranhas block, the NE trending transcurrent shear zones that branch from the east trending Patos shear zone are also associated with flat-lying mylonite belts, but these subhorizontal structures mostly exhibit extensional kinematics. Immediately north of Patos, the Rio Piranhas shear zone penetrates into the Pombal pluton (Figure 3). In continuity with the vertical mylonites of the PSZ, a flat-lying NE-SW trending mylonitic foliation develops between the PSZ and Rio Piranhas shear zone. Stretching lineations grade northward from east to NE trends. Stable biotite and amphibole and recrystallization of K-feldspars into microcline, plagioclase, and quartz within the mylonitic foliation, attest to the high temperature of deformation. Several kinematic markers (rotated porphyroclasts, S/C structures) along the vertical shear zones invariably point to a dextral sense of shear. In the low-dip foliation domain, feldspar porphyroclasts and deformed veins exhibit mostly symmetrical shapes, suggesting dominant flattening rather than noncoaxial deformation. Farther north, a complex set of NE and east trending transcurrent shear zones is connected to NW trending extensional structures gently dipping to either southwest

or northeast. The Porto Alegre shear zone (Figure 3) is the main shear zone in this sector [Hackspacher and Legrand, 1986; Trindade, 1999]. The dextral kinematics characterizing its NE and east trending branches grade into top-SW extensional deformation within the more localized NW trending shear planes, south of Caraúbas pluton (Figure 3). Another important extensional structure, the Frutuoso Gomes shear zone, runs parallel to the southern tail of the charnockitic pluton of Umarizal and merges eastward into the Brejo do Cruz dextral transcurrent shear zone. Mylonites of the Frutuoso Gomes shear zone dip to the northeast with a top-east or NE sense of shear. The presence of orthopyroxene in the gneisses and olivine in marbles, as well as widespread migmatization along the mylonitic fabric, attests to the high temperatures associated with the extensional deformation [Archanjo *et al.*, 1998]. At some places, the high-T mylonite grades into more localized greenschist mylonite and cataclasite bearing the same kinematics. To the east, the Rio Piranhas gneisses are integrated into the transpressional deformation regime prevailing in the Seridó schist belt.

### 2.4. Patos-Seridó System

[9] The Patos shear zone and the Seridó schist belt have been interpreted as a connected tectonic system [Corsini *et al.*, 1991]. Field mapping, geophysical data, and satellite images indicate that the tectonic features progressively rotate from E-W to NE-SW in perfect continuity between the shear zone and the belt [Vauchez *et al.*, 1995]. At its junction with the Seridó belt (Figure 3), the Patos shear zone (PSZ) is made of two vertical, kilometer-wide, high-temperature mylonite branches cored by migmatized gneisses and minor metasediments. The migmatites grade laterally into garnet-biotite leucogranites attesting to the high-temperature conditions reached in the PSZ. To the east, the southern branch of the PSZ grades into the Campina Grande and Remigio-Pocinhos shear zone

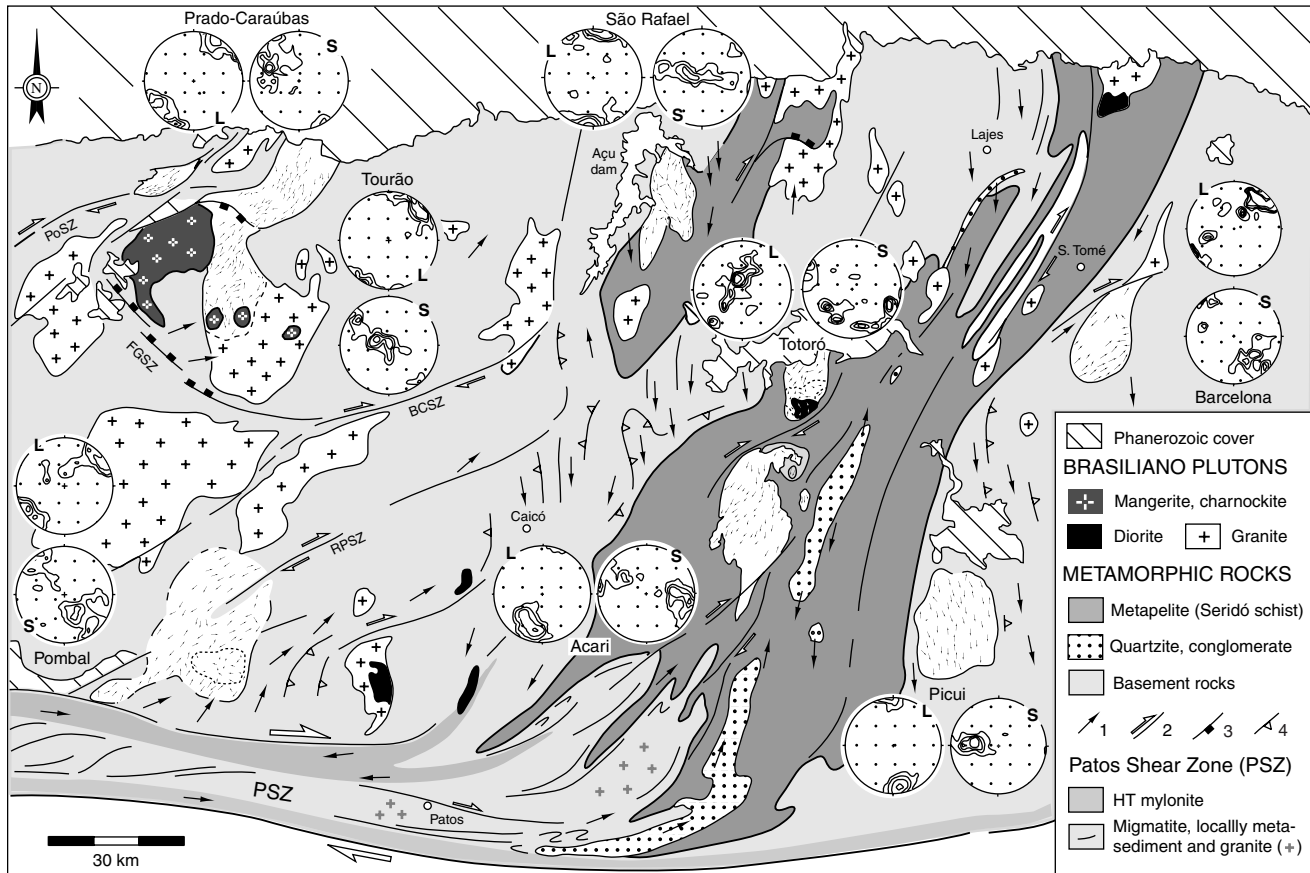


**Figure 3.** Structural map of the Seridó belt and magnetic fabric (L, lineation; S, pole of the foliation; see Table 1 for LS data sources) of granite plutons. Schmidt lower hemisphere diagrams; contours of 2, 4, 6 and 8% per 1% area. Long and short arrows inside each pluton correspond to the gentle and steep plunging magnetic lineation, respectively. The short dashed line on the plutons of Pombal and Totoró correspond to the domain of steep magnetic fabrics. Shear zones: Portalegre (PoSZ), Frutuoso Gomes (FGSZ), Brejo do Cruz (BCSZ), Rio Piranhas (RPSZ) and Patos (PSZ). Structural elements: 1, stretching/mineral lineation; 2, strike-slip shear zone and sense of movement; 3, extensional shear zone; and 4, trace of metamorphic foliation and dip.

systems [Jardim de Sá *et al.*, 1999; Vauchez *et al.*, 1995], forming the southern border of the SeB (Figure 2). The mylonitic foliation of the northern branch, while progressively rotating, develops a diffuse, anastomosing set of transcurrent shear zones inside the

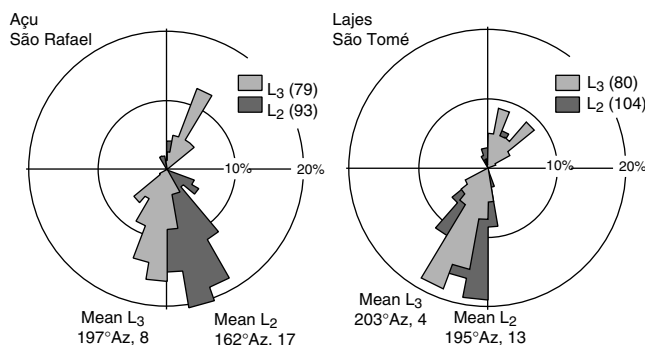


**Figure 4.** Rose diagrams of the trend of the mineral and stretching lineations on the tangential ( $L_2$ ) and transcurrent ( $L_3$ ) structures of the regions around São Rafael pluton and between Lajes-São Tomé. Number of data in parentheses. See text for discussion.

Seridó schists. The latter splay of shear zones is confined laterally, at its eastern side, by an antiform structure defined by quartzites and metaconglomerates which record a strong constrictional finite strain all along the schist belt, from Patos to Lajes (Figure 3). Finite strains computed from pebble shape ratios yield horizontal NNE-SSW trending elongation between 250% and 500% [Archanjo, 1988]. Temperatures reached along this axial zone are bracketed between 550° and 600°C [Lima, 1992], whereas temperatures in excess of 700°C were reached locally along the PSZ [Corsini *et al.*, 1998].  $^{40}\text{Ar}/^{39}\text{Ar}$  step heating analyses from different magmatic and metamorphic minerals of the PSZ-Seridó system are consistent with a hot paleogeotherm around 70°C/km followed by an unusually slow cooling history (3°–4°C/Ma) attributed to a slow rate of uplift [Corsini *et al.*, 1998].

## 2.5. Seridó Granites

[10] Potassic calc-alkaline granitoids are the most abundant magmatic rocks of the Seridó domain (Figure 2). They usually form composite batholiths, hundreds to thousands of square kilometers, that intrude both the basement rocks and the metasedimentary units. South of Patos shear zone, in the Transversal Zone,

**Table 1.** Magnetic Susceptibility and Anisotropy Parameters of Seridó Plutons<sup>a</sup>

Pluton	<i>N</i>	<i>K</i>	<i>P</i> (SD)	Lineation (AZ, Plunge)	Foliation Pole or Zone Axis (AZ, Plunge)	Reference
Prado	21	13.02	1.21 (0.11)	240°, 13	328°, 04	1
Caraúbas	71	5.59	1.27 (0.14)	034°, 02	301°, 42	1
Tourão	84	3.49	1.12 (0.06)	030°, 06	281°, 78	2
Pombal	93	8.09	1.17 (0.11)	044°, 08	042°, 07 <sup>b</sup>	3
São Rafael	51	0.98	1.11 (0.08)	183°, 00	178°, 07 <sup>b</sup>	4
Totoró	28	16.25	1.16 (0.09)	335°, 75	025°, 45 <sup>b</sup>	1
Acari	58	6.00	1.21 (0.10)	202°, 29	195°, 24 <sup>b</sup>	1, 4
Picuí	52	7.32	1.15 (0.05)	170°, 10	275°, 46	4
Barcelona	29	4.20	1.19 (0.10)	042°, 21	131°, 34	4

<sup>a</sup>Abbreviations are as follows: *N*, AMS sites; *K*, mean magnetic susceptibility ( $10^{-3}$  SI); *P*, mean anisotropy degree (SD, standard deviation), AZ, azimuth. Mean foliations are given for plutons with a well-defined maximum in foliation data, while the best zone axis is indicated for plutons whose foliations poles are distributed along a great circle. Sources are as follows: 1, this study; 2, *Trindade et al.* [1999]; 3, *Archanjo et al.* [1994]; 4, *Archanjo et al.* [1992].

<sup>b</sup>Values refer to the zone axis.

they also form large batholiths, like the Caruaru-Serra da Japcanga complex, and smaller plutons that were preferentially emplaced along contacts between the Paleoproterozoic and the Middle to Upper Proterozoic rocks (e.g., Itaporanga, Esperança, Conceição and Bodocó plutons; Figure 2). These so-called Itaporanga-type granitoids are porphyritic (K-feldspar megacrysts), usually bearing biotite and green hornblende, and have monzogranitic, granodioritic, and granitic compositions. Apatite and titanite are the main accessory minerals. Dioritic rocks of shoshonitic affinity (biotite-diorites or K-diorites) are frequently associated with the felsic rock types, showing features of mixing and mingling with them [Mariano and Sial, 1990; Neves and Mariano, 1997]. Late melts of medium- to fine-grained leucogranites generally intrude the porphyritic granites and diorites.

[11] In the SeB, diorites from the Acari pluton yield a zircon concordant U/Pb crystallization age of  $579 \pm 7$  Ma [Leterrier et al., 1994]. Indistinguishable ages of  $574 \pm 10$  Ma and  $579 \pm 4$  Ma are found in the Caraúbas and Tourão plutons, respectively [Trindade,

1999]. U/Pb ages on titanite of the São Rafael pluton are also around 575 Ma see [Sial et al., 1999]. These results suggest that the potassic calc-alkaline plutons all along the Seridó belt were emplaced during a narrow time interval. These magmas are considered to derive either from the partial melting of an enriched mafic lower crust or from a lithospheric mantle that was metasomatized during the Trans-Amazonian orogeny, as suggested by their Sm/Nd model ages (TDM) around 2.0 Ga and their very negative  $\epsilon_{\text{Nd}}$  values [Van Schmus et al., 1995].

### 3. Magnetic Mineralogy of Seridó Plutons

[12] The contrast between terranes separated by the Patos shear zone is reinforced by the magnetic signatures of the Brasileiro granites they enclose (Figure 2). Their bulk magnetic susceptibilities (*K*) have a well-defined bimodal distribution, with *K* values generally lower than  $0.5 \times 10^{-3}$  SI for plutons emplaced south of Patos shear zone (Transversal Zone) contrasting with the high *K*

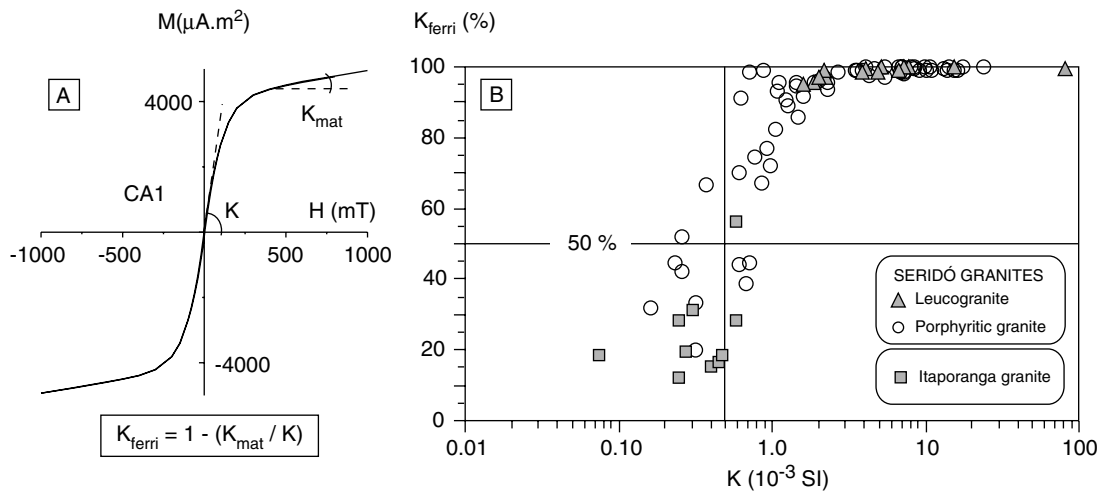


**Figure 5.** (a) Representative hysteresis loop of the porphyritic plutons of the Seridó. The vertical axis is magnetization, and the horizontal axis is applied field. Initial gradient yields bulk susceptibility (*K*), and the slope of the curve at fields above 500 mT is proportional to the matrix susceptibility (*K<sub>mat</sub>*). The ferrimagnetic susceptibility (*K<sub>ferri</sub>*) is calculated by subtracting *K<sub>mat</sub>* from *K*. (b) For the Seridó plutons, *K<sub>ferri</sub>* decreases considerably below susceptibility values of  $10^{-3}$  SI.

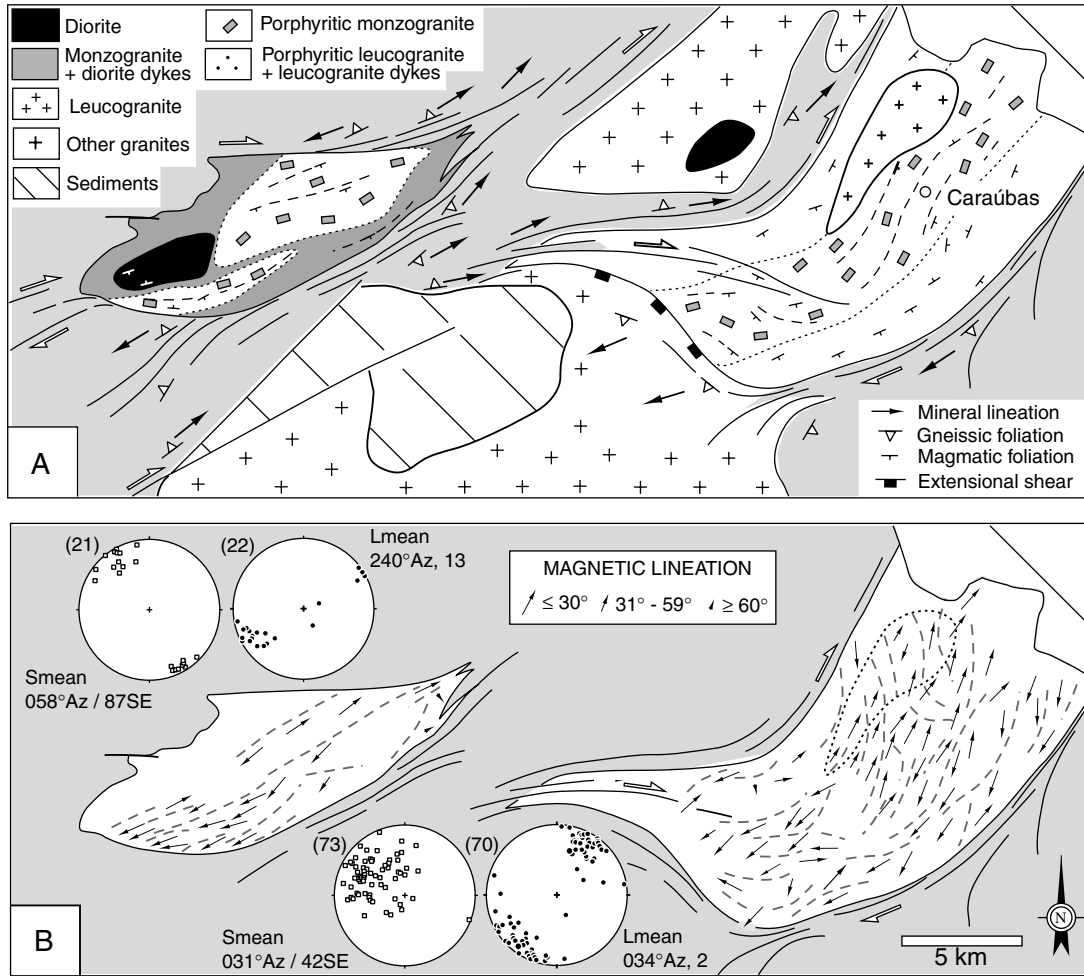


**Figure 6.** (a) Geological map and (b) magnetic fabric of the Prado-Caraúbas Complex. The trace of the magnetic foliation is represented by long dashed lines. Note the foliation transecting the contact (short dashed line) of the leucogranite in the Caraúbas pluton. The magnetic lineation ( $L$ ) and pole of magnetic foliation ( $S$ ) are shown on the Schmidt diagrams, lower hemisphere.

values, up to  $10^{-2}$  SI, that characterize the plutons of the Seridó [Archanjo *et al.*, 1992] (Table 1). The origin of the high and low values of  $K$  of the plutons separated by a shear zone is not well understood. Melting of different source rocks and/or contamination of the magma during emplacement may concur to the regional variability of  $K$ . Contamination is a plausible hypothesis since the aeromagnetic regional maps show that the remanent magnetization of the Seridó rocks is higher than the Transversal Zone. Melting of the host rocks during magma ascent and emplacement would increase the amount of magnetic minerals in the magma, hence increasing the bulk susceptibility of the granites of the SeB.

[13] In the porphyritic granites, opaque minerals represent  $\sim 0.5\%$  of rock volume, comprising predominantly euhedral primary crystals of magnetite with mean grain-sizes of  $20\ \mu\text{m}$  in close association with titanite, biotite, and amphibole [Archanjo *et al.*, 1995; Trindade *et al.*, 1999]. Correspondingly, these rocks give signatures typical of multidomain, Ti-poor titanomagnetite to pure magnetite, as characterized by their Curie temperatures between  $565^\circ$  and  $580^\circ\text{C}$ , low-field saturation of remanence in acquisition curves, and narrow-waisted hysteresis loops [Trindade, 1999]. Minor amounts of fine-grained needle-shaped magnetites ( $1\text{--}5$

$\mu\text{m}$  long), observed within biotite and chlorite cleavages, derive from late hydrothermal alteration of Fe-rich phyllosilicates [Galindo *et al.*, 1995; Trindade *et al.*, 1999]. Hematite was also found in some samples as a secondary phase from alteration of magnetite [Archanjo *et al.*, 1995], usually occurring either within microcracks or at the borders of magnetite grains, forming thin lamellae parallel to  $\{111\}$  planes of magnetite. No sulfides have been observed, either magnetically or by microscopic study.

[14] The contribution of magnetite to the bulk susceptibility of the granites has been defined by means of hysteresis loops (Figure 5a). The sum of diaferromagnetic, paraferromagnetic, and anti-ferromagnetic contributions, named matrix susceptibility ( $K_{\text{mat}} = K_{\text{dia}} + K_{\text{para}} + K_{\text{ant}}$  [Rochette, 1987]), can be determined at high induced magnetic fields after saturation of the ferrimagnetic fraction. Assuming that  $K_{\text{ant}}$  is constant through all applied fields, or is negligible, the contribution of the ferrimagnetic fraction ( $K_{\text{ferri}}$ ) to the bulk susceptibility is easily calculated by subtracting  $K_{\text{mat}}$  from  $K$  in the hysteresis loop (Figure 5a). This procedure was applied to 123 samples of Itaporanga-type granites from the Acari, Barcelona, Gameleiras, Pombal, Caraúbas, Prado, and Tourão plutons. The percentage of ferrimagnetic contribution ( $K_{\text{ferri}}\%$ )

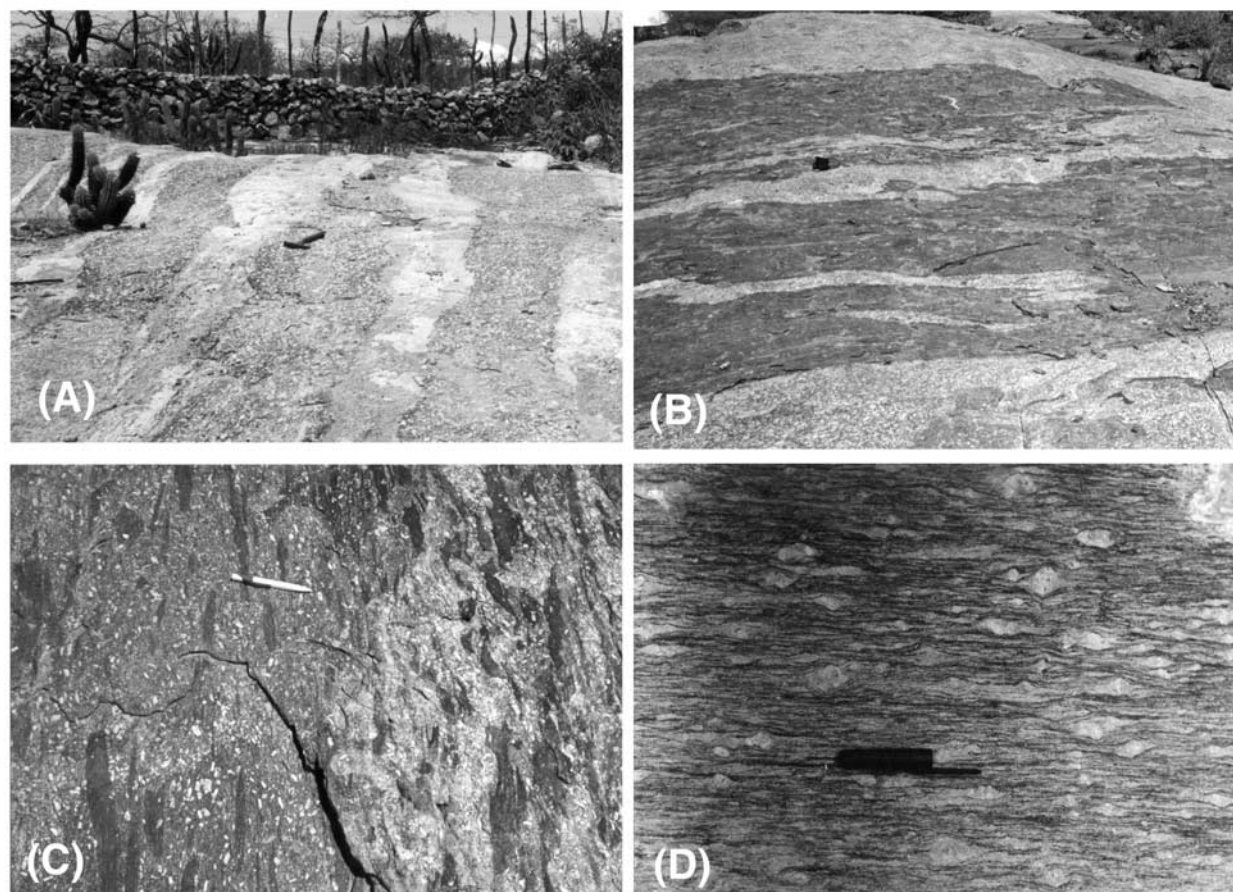


**Figure 7.** Deformational and magmatic features of the plutons of Caraúbas (Figures 7a and 7d) and Prado (Figures 7b and 7c). (a) Leucogranite dykes intrusive in porphyritic granite. (b) Diorite (dark bands) and porphyritic granite dipping steeply parallel to the pluton elongation. (c) Detail of Figure 7b, showing disrupted dark lenses of diorite included in layers of monzodiorite (left) and granite (right). Euhedral to subhedral megacrysts of feldspar occur in all facies suggesting that these magmas were partially commingled. (d) Augen mylonite formed by shearing of a porphyritic granite. The sense of movement is top to northeast (right). Section normal to foliation (vertical) and parallel to stretching lineation.

has been plotted against  $K$  ( $10^{-3}$  SI) for each specimen (Figure 5b). In all leucogranites the ferrimagnetic contribution ranges predominantly between 96% and 100% in accordance with the small amount of paramagnetic minerals in these very leucocratic rocks. In the porphyritic granites, where biotite and amphibole may exceed 20% in modal composition, the values of  $K_{\text{ferri}}\%$  vary more widely, between 37% and 100%, usually above 50%. By contrast, 11 samples of the Itaporanga granite, which belongs to the Transversal Zone (Figure 2), give  $K_{\text{ferri}}\%$  generally below 40%, values which are consistent with the low content of ferrimagnetic minerals observed in the plutons south of the Patos shear zone.

#### 4. Internal Fabrics of the Granite Plutons

[15] Nine plutons from the Seridó domain have been studied by means of AMS (Table 1 and Figure 3). Four of them belong to the Rio Piranhas block (Caraúbas, Pombal, Prado, and Tourão), and five belong either to the Seridó schist belt (Acari, São Rafael, and Totoró) or to its eastern border (Picuí and Barcelona). In addition to

an overview of granite fabric patterns in the whole Seridó domain, we give a description for one well-dated magmatic complex within each sector, namely the Prado-Caraúbas complex in the Rio Piranhas block, and the Acari-Totoró complex in the schist belt.

##### 4.1. Rio Piranhas Block

[16] In the western part of the Rio Piranhas block, the NE trending structures and some extensional NW trending ones enclose and penetrate into several granite plutons that were emplaced along a roughly north trending axis (Figure 3). High- $K$  calc-alkaline granites form the largest plutons along this axis, namely, Pombal, Tourão, and Caraúbas (Figure 3). Charnockitic alkaline magmas such as the Umarizal pluton ( $\sim 200$  km<sup>2</sup>) and small stocks intruding the Tourão and Serra do Lima granite plutons (Figure 3), were also emplaced along this axis, controlled by the NW trending extensional Frutuoso Gomes shear zone [Archanjo *et al.*, 1998]. All the plutons studied in this domain have consistent fabric patterns, particularly subhorizontal NE trending lineations (Table 1), parallel to the stretching directions

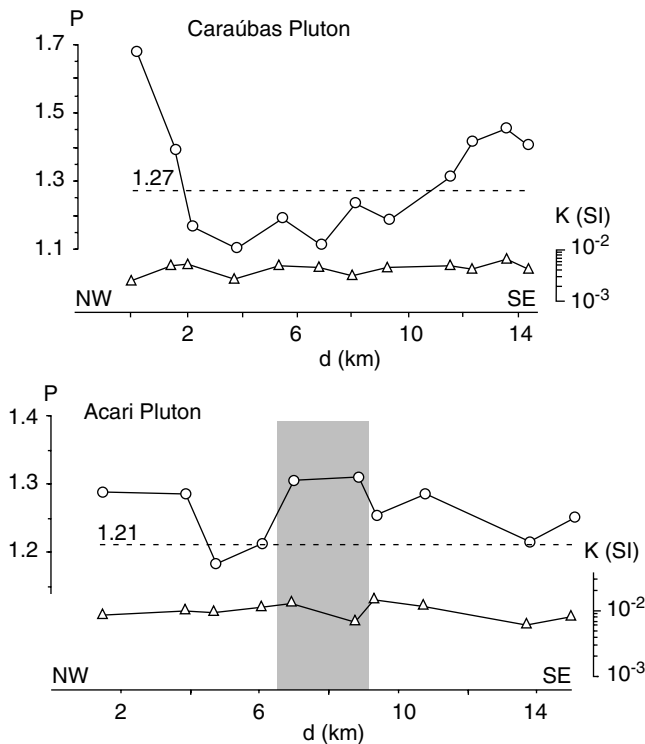


**Figure 8.** Variation of the mean anisotropy degree ( $P$ ) of stations along NW-SE traverses across the (a) Caraúbas and on (b) Acari plutons. The mean anisotropy of each pluton (dashed line), and the variation of susceptibility of corresponding stations are indicated.  $P$  increases on the border of the Caraúbas pluton and on the shear zone that crosscuts the Acari pluton (shaded area).

measured along the ENE to NE trending shear zones developed in the country rocks.

**4.1.1. Prado-Caraúbas complex.** [17] The northeasternmost segment of the Porto Alegre shear zone spreads out into a set of dextral east and NE trending mylonite belts, tens to hundreds of meters wide, that transform the igneous porphyritic texture of Caraúbas and Prado plutons into typical augen gneisses. Gneissic foliations have steep to moderate dips, and lineations are close to horizontal. An ESE trending branch of this shear zone penetrates into the Caraúbas pluton and also marks the northern boundary of the Tourão pluton (Figure 6a). There, the ESE trending mylonitic foliation dips around  $40^\circ$  to the southwest, and the stretched feldspars plunge almost down-dip, i.e., to the west-southwest, with a top-SW sense of shear indicating an apparent extensional kinematics. The Prado ( $\sim 60 \text{ km}^2$ ) and Caraúbas ( $\sim 250 \text{ km}^2$ ) plutons were emplaced in the northwest and southeast of the Portalegre shear zone, respectively (Figure 6a). They are characterized by central porphyritic monzogranites bordered by sets of leucogranitic (Caraúbas) and dioritic (Prado) dykes up to 500 m wide, forming peculiar layering features (Figures 7a and 7b). Mafic enclaves suggestive of disrupted dykes occur parallel to the layers of monzogranite and monzodiorite (Figure 7d). Dioritic rocks locally form small stocks as observed in the southwest part of Prado. A small sheet-like leucogranite body ( $\sim 20 \text{ km}^2$ ) occurs between the coarse-porphyritic core of Caraúbas and its border (Figure 6a). Farther northwest, approaching the host rock contact,

the porphyritic granites are transformed into augen mylonites (Figure 7d), and dykes are folded and boudinaged. The distribution of the magmatic facies within them seems to be controlled by the Portalegre shear zone. The shapes of both plutons and aligned igneous feldspars, mafic, enclaves, and dykes all have NE trends, except on the southern part of Caraúbas where the magmatic foliation dips moderately southwestward.

**4.1.2. Magnetic fabric.** [18] Samples from 21 sites of Prado and 71 sites of Caraúbas were studied for their AMS according to the procedure described by Bouchez [1997]. At each site, two to four oriented cylindrical cores were drilled, taking care to avoid contacts with dykes or veins, or with places affected by hydrothermal alteration or fractures. The principal axes of the anisotropy ellipsoid ( $K_1 \geq K_2 \geq K_3$ ) are calculated from four to eight specimens per site. The long axis,  $K_1$ , is the magnetic lineation, and the short axis,  $K_3$ , is perpendicular to the magnetic foliation. The anisotropy degree, or eccentricity of the ellipsoid, is given by  $P = K_1/K_3$  ranging from 1 (sphere, isotropic) upward.

[19] The mean magnetic susceptibility  $K = 1/3(K_1 + K_2 + K_3)$  is higher for Prado ( $13.02 \times 10^{-3} \text{ SI}$ ) than for Caraúbas ( $5.59 \times 10^{-3} \text{ SI}$ ). Mean  $P$  values are similar for both plutons ( $P = 1.21$ , s.d. = 0.11 for Prado, and  $P = 1.27$ , s.d. = 0.14 for Caraúbas). They strongly reflect the strengths of the rock fabrics, as attested in Caraúbas by plotting the mean  $P$  values from 12 sites located along a NW trending 13 km long traverse (Figure 8a). For almost constant  $K$  values around the mean susceptibility, the anisotropy degree increases from pluton center to its borders, correlating with the amount of strain recorded by the rocks. Along the traverse, the weak mineral fabrics, associated with magmatic to submagmatic

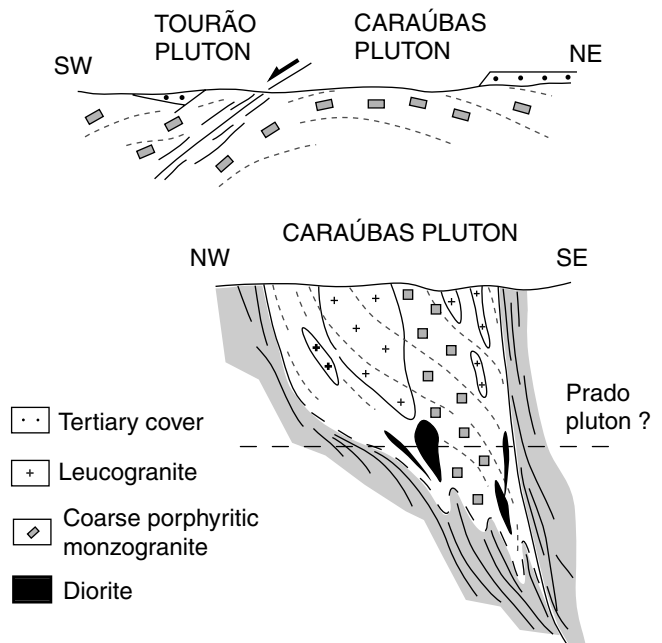


**Figure 9.** Schematic cross sections (not in scale) perpendicular (NW-SE) and parallel (NE-SW) to the elongation of the Caraúbas pluton. A possible section of the Prado pluton would correspond to the deepest parts of the chamber where the foliation should be nearly parallel to the igneous contacts. See text for discussion.



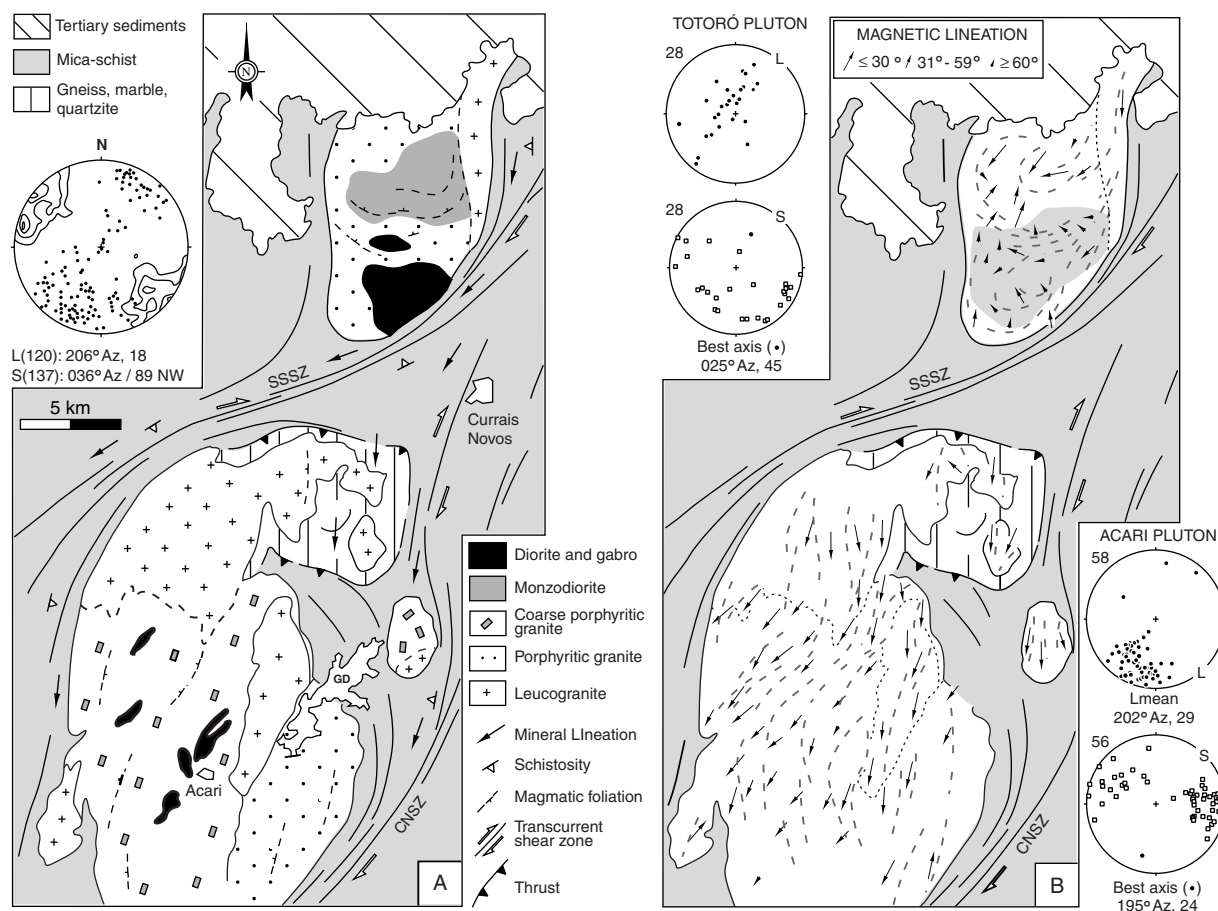


**Figure 10.** (a) Geological map and (b) magnetic fabric of the Acari-Totoró Complex. CNSZ and SSSZ are the Currais Novos and Serra da Sarama shear zones. (A) The host rock mineral lineation (L) and contour of the pole of schistosity (S) are shown in the Schmidt diagram, lower hemisphere (upper left). Contours of 2, 4, 6 and 8% per 1% area. (B) The shaded area in the Totoró pluton corresponds to the steep dipping fabric domain. The trace of the magnetic foliation is represented by dashed long lines. The magnetic lineation (L) and pole of magnetic foliation (S) are shown on the Schmidt diagrams, lower hemisphere.

type microstructures, grades to high-T mylonites where approaching the shear zones [Trindade, 1999].

[20] The magnetic lineations plunge gently to the southwest in Prado (mean at 240° azimuth (AZ), 13) or to the northeast in Caraúbas (mean at 034° AZ, 02) (Figure 6b). The magnetic foliations have NE strikes and dip steeply in Prado and moderately (mean at 42° to SE) in Caraúbas. In some places of Caraúbas the foliation is oblique to the compositional boundaries (Figure 6b). For example, in the central and northern sectors of this pluton, magnetic foliation trajectories transect the contact between the leucogranite sheet and the coarse porphyritic facies, and the NE trending lineations plunge nearly down-dip. In the south the foliations turn progressively from NE to ESE in strike and crosscut the contact between the porphyritic and the leucogranite types. There, the magnetic fabric becomes parallel to the extensional branch of the Portalegre shear zone. In the footwall of this extensional branch, formed by the Caraúbas pluton itself, the magnetic lineations plunge to the southwest. This magmatic fabric keeps the same orientation when changing into a solid-state gneissic fabric toward the contact with the Tourão pluton [Trindade et al., 1999].

A NE trending cross section of Caraúbas (Figure 9), parallel to the magnetic lineations, shows that these lineations form a continuous arcuate pattern along Caraúbas and Tourão that calls for a south-westward extension of the whole massif. In a schematic NW-SE cross section of Caraúbas, magnetic foliations display an asymmetric pattern, parallel to the compositional contacts near to the steep walls of the pluton but transecting them in its core. Figure 9 also tentatively depicts a more mafic, deep-seated portion of this pluton, an equivalent to the diorite bodies that outcrop in the Prado pluton.

## 4.2. Seridó Schist Belt

[21] The plutons of the schist belt display somewhat different fabric patterns (Figure 3). The lineations remain close to the horizontal on average, but their trends are N-S in São Rafael and NNE-SSW in Acari (Table 1). In the São José de Campestre block the fabrics of the plutons that intrude close to the contact with the metasediments systematically follow the host rock structures. The Picuí pluton was emplaced in a sector of the basement characterized by low-dip foliations. Correspondingly, pluton foliation dips

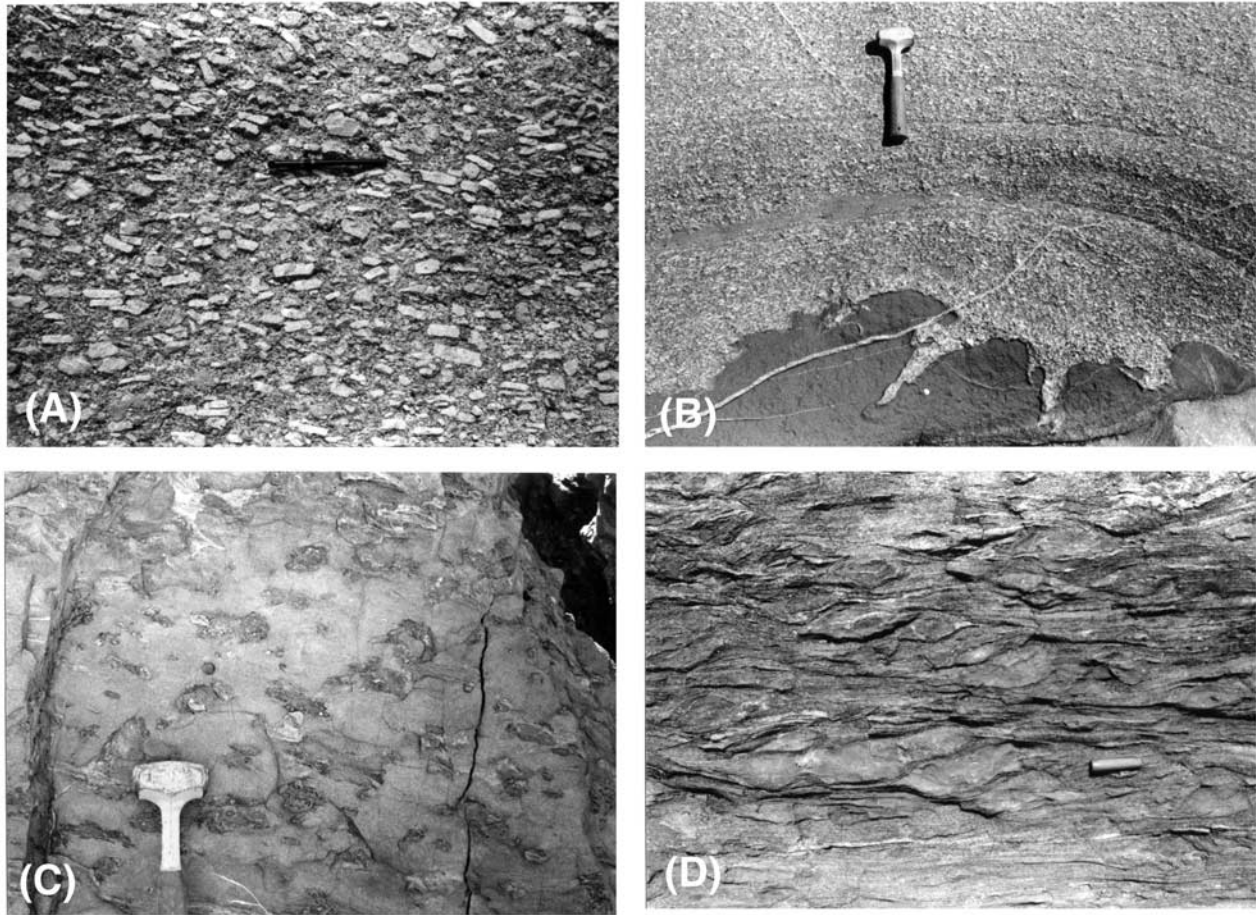


**Figure 11.** Deformational and magmatic features of the plutons and host rocks of the Seridó. (a) Alignment of megacrysts of K-feldspar trending to NNE on the Acari pluton. This fabric type is normally observed on its whole porphyritic facies. (b) Fine magmatic layering dipping steeply (head of hammer points to north) in the Totoró pluton. Flame-like leucocratic veins pierce the mafic enclave (dark) suggestive of a load-cast structure formed by compaction of magmas of different viscosities. (c) Lineation of ellipsoidal cordierite nodules plunging to SSW, viewed on the plane of foliation of a metapelite near the southeastern contact of the Totoró pluton. (d) Asymmetric porphyroblasts of cordierite on the Currais Novos shear zone. The S-C planes and porphyroblast strain shadows define a dextral (top to NNE) movement. Section normal to the foliation (vertical) and parallel to the stretching lineation.

gently to the east, and the lineations plunge regularly to the SSE. The pluton of Barcelona, emplaced close to NE trending shear zones, shows NE trending lineations and predominantly steep NW dipping foliations. In contrast to these pluton-host rock conformable fabrics, the Totoró pluton, located directly to the north of Acari, has steep lineations and inward dipping foliations. Steeply plunging lineations are also observed in the Rio Piranhas block, at the southern tip of the Pombal pluton [Archanjo *et al.*, 1994] (Figure 3).

**4.2.1. Acari-Totoró magmatic complex.** [22] The N-S elongate Acari (~250 km<sup>2</sup>) and Totoró (~100 km<sup>2</sup>) plutons intrude metapelitic country rocks (Figure 10a). Acari is a porphyritic monzogranite, including lenses of diorite in its center and a porphyritic granite on its eastern side. Totoró is dominantly composed of porphyritic granite and monzodiorite, including small stocks of diorite and gabbro. Sheet-like bodies of leucogranite intrude both plutons and their country rocks in the north of Acari

and in the east of Totoró. In Acari, the K-feldspar megacrysts display well-defined shape fabrics parallel to pluton elongation (Figure 11a). In its southern tail, a high-temperature gneissic fabric is marked by stretched feldspar megacrysts tailed by strain shadows and infilled with recrystallized quartz and oligoclase. Late veins of aplite and pegmatite are folded, display pinch-and-swell structures, or form isolated boudins parallel to the foliation marked by flattened biotite clusters and quartz. In Totoró a magmatic banding is commonly defined by centimetric layers of hornblende and biotite ( $\pm$  clinopyroxene) alternating with feldspar layers, particularly at the contacts with the diorite stocks (Figure 11b). These contacts are magmatic, as attested by flame-like leucocratic material penetrating into the mafic rocks. Such features are attributed to compaction between magmas having different solid fractions, hence different viscosities.

[23] The metamorphic aureole in the host metapelites west of Acari increases from low-grade (muscovite + chlorite) at a distance

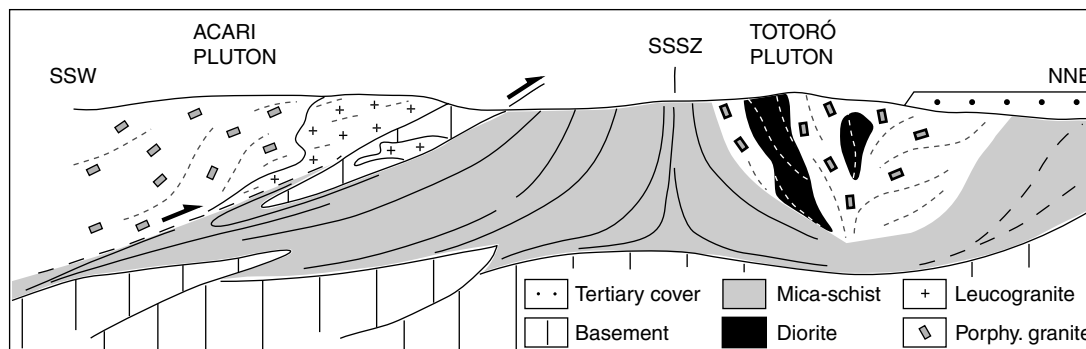


**Figure 12.** Schematic cross section (not in scale) parallel to the elongation direction of Acari and Totoró plutons. The shape of the Totoró pluton in-depth, the termination of the Serra da Sarambaia shear zone (SSSZ) at depth, and the structure on the top of the basement are speculative.

of 10 km from the pluton, to high grade with sillimanite and cordierite assemblages near the contact. Orthopyroxene is also observed in the metapelites at contact with gabbros and within xenoliths of the Totoró pluton. Thermobarometric determinations around the Acari-Totoró complex yield peak temperatures of 630°C for depths of 12–15 km [Lima, 1992]. Foliations around the plutons dip steeply, except in the north of Acari where a thrust-fault dipping moderately to the south carries up Paleoproterozoic orthogneisses and older metasediments upon the Seridó schists (Figures 10 and 12). Stretching and mineral lineations plunge southwestward everywhere around the plutons (Figure 11c). In Acari the stretching lineations become vertical at the contact between the leucogranite and the host rocks near the Gargalheiras dam, and in the northern border of the pluton. In lower grade away from the plutons, a steep axial-planar foliation, marked by biotite flakes cutting across the bedding of metarhythmites, defines a NE plunging intersection lineation. Where approaching the shear zones, the foliation becomes severely transposed, and cordierite becomes synkinematic within dextral S/C surfaces (Figure 10d). K-feldspar and sillimanite have recrystallized in strain shadows, attesting to the high temperatures reached during shearing. The main shear zones around the plutons are the NNE trending Currais Novos shear zone and the NE trending Serra da Sarambaia shear zone (Figure 10). The latter seems to vanish southwestward into the low-grade metapelites. The Currais Novos shear zone, on the other hand, can be traced to the south as a set of high-strain zones merging into the Patos shear zone (Figure 3).

**4.2.2. Magnetic fabric.** [24] The AMS of Acari and Totoró have been determined from 58 and 28 sampling stations, respectively. The mean magnetic susceptibility is higher in Totoró ( $K = 16.25 \times 10^{-3}$  SI) than in Acari ( $K = 6.00 \times 10^{-3}$  SI). The anisotropy magnitudes ( $P$ ) are indistinguishable (Acari, mean  $P = 1.21$ , s.d. = 0.10; Totoró, mean  $P = 1.16$ , s.d. = 0.09). The magnetic fabric of Acari is relatively simple: Foliations dip steeply to moderately around a zone axis at 195°AZ, 24, whereas the lineations plunge SSW (mean at 202°AZ, 29) parallel to the zone axis. The lineations define a rough sigmoidal pattern consistent with dextral shear parallel to the NE trending shear zones developed in the country rocks. Contrasting with Carábas, the highest degree of anisotropy is recorded in the center of Acari, within a corridor oblique to pluton elongation (shaded in Figure 8b) where shear deformation was localized during pluton

crystallization (Figure 10b). This overall magnetic fabric pattern, very similar to the metamorphic fabric imprinted in the host rocks, indicates that the pluton and its host rocks were deformed together by the same shear zone system. The magnetic fabric of Totoró is very different since most lineations plunge steeply (>60°, shaded in Figure 10b), suggesting that a steep magma flow has been frozen-in during emplacement. The foliations mainly dip inward and form concentric patterns in the center of the pluton that grade into parallelism with the contacts toward them. Despite their down-dip plunges, the lineations are distributed along a plane almost parallel to pluton elongation. A tentative cross section parallel to lineation is shown in Figure 12, where the southward plunges of the Acari lineations are considered to belong to a frontal ramp including a slice of basement rocks thrust over the metapelites. This cross section also represents leucogranitic melts occurring preferentially along the ramp contact and intruding the allochthonous basement. Note that near the Serra da Sarambaia shear zone the foliation is upright, but it is supposed to flatten downward where approaching the basement.

## 5. Discussion

### 5.1. Significance of Magnetic Fabrics in the Granites

[25] The magnetic properties of the granitic plutons are mainly carried by nearly pure, multidomain magnetite grains whose shapes control the magnetic fabric [Archanjo et al., 1995; Grégoire et al., 1998; Launeau and Cruden, 1998]. In a few sites having susceptibilities lower than  $0.35 \times 10^{-3}$  SI, the contribution of the paramagnetic silicates (biotite and hornblende) to the bulk susceptibility may reach 70%. However, even in these weakly magnetic rocks a hysteresis can still be detected, pointing to the presence of mainly fine-grained ferrimagnetic particles. Ilmenite, which is paramagnetic at room temperature, and hematite, which has a strong anisotropy on the basal plane, occur as traces and do not significantly contribute to the magnetic anisotropy. Parallelism between the AMS axes and the mineral rock fabrics in the granites has been tested in three different ways: (1) at the scale of a whole pluton, by comparing the magnetic fabric patterns with field measurements [Archanjo et al., 1992; Trindade, 1999], (2) at the sample scale, by comparing the AMS with the shape fabrics of magnetite and biotite by means of image analysis [Archanjo et

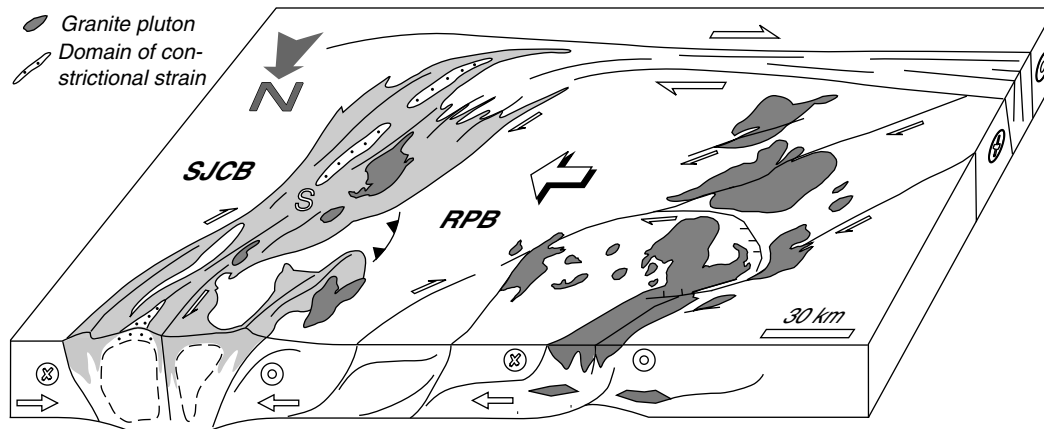


**Figure 13.** Proposed geodynamic scenario for the Seridó belt (SeB) at the time of the emplacement of the Itaporanga type plutons. RPB, S, and SJCB are the Rio Piranhas Block, Seridó schist belt, and São José de Campestre block, respectively. See text for discussion.

*al.*, 1995], and (3) by comparing the AMS fabric with the fabric of coarse-grained magnetite using the anisotropy of partial anhysteretic remanence at low coercivities [Trindade *et al.*, 1999].

**5.1.1. Highly coupled fabrics.** [26] Except for Totoró and part of Pombal, where steep fabrics are recorded, the plutons and their host rocks share similar fabrics all along the SeB. They are characterized by (1) gently plunging lineations parallel to the regional stretching direction whether trending north (central portion of the belt) or NE (Rio Piranhas block) and (2) foliations dipping at varying angles and oriented around a zone axis parallel to mean lineation and pluton elongation, or dipping rather gently where the host regional rocks record a low-angle fabric. These features are typical of syntectonic intrusions where the magmatic host rock system is mechanically coupled at high temperature. A closer inspection of the internal contacts in Caraúbas and Acari plutons reveals that the foliation transects the contacts between the porphyritic and leucogranite rock types (Figures 6 and 10). In fact, the leucogranites represent the latest magmatic pulses, possibly due to partial melting of the host rocks, as suggested by their peraluminous character and by the presence of muscovite, garnet, and tourmaline. The continuity of fabric between these rocks and the other rock types inside the plutons demonstrates that they were deformed together in the magmatic state, with small viscosity contrasts between them. Hence, the internal structures of the Seridó plutons were acquired within their present setting sites, after the different magma batches were emplaced, but before the plutons became completely crystallized. When present, solid-state deformation is concentrated along narrow shear zones predominantly at the borders of the intrusions.

**5.1.2. Uncoupled fabrics.** [27] The dominantly high temperature of the whole crust of the SeB allowed the granite magmas to deform long enough in time within their enclosing ductile host, under grain-supported flow [Vigneresse and Tikoff, 1999]. This explains why syntectonic fabrics, characterized by subhorizontal stretching patterns, are ubiquitously recorded in the plutons. Nonetheless, zones of steep fabrics have been identified in Pombal and Totoró. The Totoró pluton, with its concentric and inward dipping foliations, contrasts sharply with the structural pattern of Acari, which belongs to the same schist-belt domain.

This difference is attributed to the more mafic composition of Totoró compared to the dominantly felsic nature of Acari: Since solidus temperatures are higher for undersaturated mafic magmas [see Johannes and Holtz, 1996], the time span for these magmas to stop deforming under grain-supported flow may have been shorter than for felsic magmas. The fabrics of Totoró were therefore frozen-in during magma ascent. The same line of reasoning also applies to some sites of Acari, where mingled mafic rocks and agmatitic-like diorite enclaves exhibit sharp contacts with the host porphyritic granite and thus also point to a higher viscosity and more advanced crystallization of diorites than the enclosing granites. By contrast, the mafic rocks of Prado, which do not retain any fabric related to magma ascent, were readily incorporated in the regional shear strain. The Pombal pluton, although dominantly granitic in composition, also shows ascent-related fabrics along with typical magmatic microstructures. Here the preservation of steep fabrics is attributed to magma emplacement within a low strain area partitioned between the Patos and Rio Piranhas shear zones [Archanjo *et al.*, 1994].

## 5.2. Regional Tectonic Model

[28] The fabric patterns observed in different areas of the SeB suggest a partitioned strain consisting of transpression in the schist belt, transtension in the western part of the Rio Piranhas block (RPB), and a transfer zone all along the Patos shear zone (PSZ) (Figure 13). The similar U/Pb ages obtained for potassic calc-alkaline plutons along these three domains indicate that their emplacement took place, and their internal structures were acquired, simultaneously at around 580 and 575 Ma. The fabrics of granite plutons in Figure 3 therefore represent a snapshot of the regional deformation pattern over a large subhorizontal section of a “hot” midcrust between the Patos shear zone to the south, and the Potiguar Basin to the north.

**5.2.1. Transpressional domain.** [29] The transpressive deformation of the central part of the SeB was basically controlled by the Patos shear zone that pushed the Rio Piranhas Block (RPB) to the east. The presence of a low-strength domain explains the transfer of movement and the concentration of deformation along the schist belt [Tommasi and Vauchez, 1997].

This general model accounts for dextral shearing, lateral shortening, and strong strike-parallel subhorizontal stretch in the leading edge of the RPB (Figure 13). Correspondingly, the syntectonic granites have lineations close to the direction of stretching and fold axes. The typical fabric patterns in this sector, defined by foliations distributed around the mean lineation, agree with the strong constrictional deformation recorded along the hinges of the antiformal domes in the axial zone of the SeB. The strongly oblique stretch on the metamorphic domes within the metasediments and along the subhorizontal structures at the contact with the basement reflects the lateral expulsion of rocks by impingement of the RPB. Emplacements of Acari and Totoró plutons can also be attributed to their upward extrusion, in agreement with dynamic models of ductile transpressive zones that predict a progressive change of flow lines from horizontal to vertical [Robin and Cruden, 1994]. This upward migration of magma was well recorded inside Totoró by its steep lineations dispersed along a plane perpendicular to the shortening direction of the belt (Figure 10b). It is worthwhile to note that the Acari pluton occupies the flattened domain in between the Serra da Sariema and Currais Novos shear zones (Figure 3), indicating that the pluton was in compression when its magmatic fabric was formed. Eastward, in the São José de Campestre block, the foliation and lineation also rotate to NE-SW in Barcelona and to N-S around Picuí (Figure 3). Farther east, N-S escape was accommodated along conjugate pairs of NW trending sinistral and NE trending dextral shear zones, the former providing room to the emplacement of alkaline pluton of Japi [Jardim de Sá et al., 1999].

[30] The tectonic framework of the transpressional domain is consistent with models that integrate the  $L_2$  and  $L_3$  lineations in a monocyclic deformational event [Archanjo et al., 1992; Caby et al., 1995; Hackspacher et al., 1997]. In such a scenario, the  $L_2$  stretching lineation would occur along the NW trending branch of a conjugate shear zone system formed when a weak zone (metapelitic belt) is squeezed between a stiffer (basement) domain [Cosgrove, 1997]. Localization of deformation along high-strain NE trending corridors in the latest deformational stages must rotate and transpose  $L_2$  to the  $L_3$  stretching direction.

**5.2.2. Rio Piranhas transtensional domain.** [31] A bulk eastward movement of the Rio Piranhas block was not homogeneously distributed internally. In the front of the block the strain was partitioned in transcurrent shearing and lateral escape as described in section 5.2.1, while its western border is characterized by widespread crustal extension. The transtensional structures can be traced at depth as forming the strong flat-lying reflectors observed in deep-seismic profiles obtained just to the north, beneath the Potiguar basin [Matos, 1992], whose basement corresponds to the middle to lower crust exposed in the block of Rio Piranhas. The several NE and east trending transcurrent shear zones that branch from Patos must therefore also flatten at depth and branch into these flat-lying structures (Figure 13).

[32] In the Rio Piranhas Block, the flat-lying structures change in vergence on sides of the north trending axis where granite plutons were preferentially emplaced. The mechanism of emplacement of this voluminous magmatism is illustrated by the Prado and Caraúbas plutons. These plutons were formed by the successive

intrusion of vertical sheet-like bodies of varied composition, comprising diorites, porphyritic granites and leucogranites, along the transtensional jog formed by the NE and east trending branches of the Porto Alegre shear zone. The continuity between the magmatic and host rock fabrics agrees with an emplacement of the mafic and felsic magmas controlled by the transtensional deformation. The low-to moderate-dipping foliation of the Tourão pluton would thus record the partitioning of strain between the flat ramps and the steep shear zones, a feature also observed on the southern border of the Pombal pluton [Archanjo et al., 1994]. In this scenario, the continuous rise of the westernmost Rio Piranhas block, driven by the upwelling of such a voluminous granitic magmatism, would be dissipated by the extensional deformation, leading to crustal thinning along this axis where the charnockite rocks of Umarizal were finally emplaced. This axial zone of the Rio Piranhas block may therefore correspond to the deep-crustal section of an intracontinental rift zone. This ancient crustal feature may have also controlled the opening of the small, intracontinental Mesozoic rift system distributed along Caraúbas-Pombal axis [see Matos, 1992].

## 6. Conclusions

[33] The highly coupled granite fabric patterns that characterize the different areas of the Seridó belt are here used to trace the Brasiliano strain partitioning over more than 45,000 km<sup>2</sup> in northeastern Brazil. These fabric patterns record the finite strain acquired in the time interval between the complete assembly of magma batches and the end of their grain-supported flow. Hence, they record a narrow time interval of the Brasiliano deformation history, around 575 Ma, corresponding to the peak of regional metamorphism. During this rather short period of time, deformation was concentrated either inside the magma bodies or along the shear zones. However, in contrast to the heterogeneous deformation recorded in the ductile country rocks, granite magmas show remarkably homogeneous fabrics.

[34] Differences in granite fabrics allow distinguishing between a transtensional domain in the west and a transpressional domain in the east, acting simultaneously. They formed a mechanically coupled tectonic system linked to a vertical east trending transfer zone (Patos). This regional partitioning of strain probably resulted from the different rheological behaviors along the domains. The bulk eastward movement of the Rio Piranhas Block would have been driven by the large granitic magmatism emplaced along its western border as well as the movement of the Patos shear zone. In the leading edge of the block, some of the squeezed rocks were dragged into the transfer zone, and some were accommodated by thrusts. The shortening of the basement in the central portion of the belt would allow upward extrusion of granite and diorite magmas that finally crystallized adjacent to the metasedimentary cover.

[35] **Acknowledgments.** This work has been sponsored by the Brazilian Agencies, CNPq (grant 300889/96-8) and FAPESP (grant 95/8399-0). We acknowledge helpful discussions on the regional geology of the Seridó belt with many people over the years, including Alain Vauchez, Benjamim Bley de Brito Neves, Emanuel Jardim de Sá, and Renaud Caby, but remaining misperceptions are our responsibility. Careful review by David Evans is much appreciated and helped to improve the paper.

## References

- Archanjo, C. J., A deformação constriccional nos metaconglomerados da Faixa Seridó, in *Congresso Brasileiro de Geologia*, 35th, vol. 5, pp. 2240–2247, Soc. Brasileira de Geol. Belém, Brazil, 1988.
- Archanjo, C. J., and J. L. Bouchez, Le Seridó, une chaîne transpressive dextre au Protérozoïque supérieur du Nord-Est du Brésil, *Bull. Soc. Géol. Fr.*, 162, 637–647, 1991.
- Archanjo, C. J., P. Olivier, and J. L. Bouchez, Plutons granitiques du Seridó (NE du Brésil): Écoulement magmatique parallèle à la chaîne révélé par leur anisotropie magnétique, *Bull. Soc. Géol. Fr.*, 163, 509–520, 1992.
- Archanjo, C. J., J. L. Bouchez, M. Corsini, and A. Vauchez, The Pombal granite pluton: Magnetic fabric, emplacement and relationships with the Brasiliano strike-slip setting of NE Brazil (Paraíba State), *J. Struct. Geol.*, 16, 323–335, 1994.
- Archanjo, C. J., P. Launeau, and J. L. Bouchez, Magnetic fabric vs. magnetite and biotite shape fabrics of the magnetite-bearing granite pluton of Gameleiras (Northeast Brazil), *Phys. Earth Planet. Int.*, 89, 63–75, 1995.
- Archanjo, C. J., J. W. P. Macedo, A. C. Galindo, and M. G. S. Araújo, Brasiliano crustal extension and emplacement fabrics of the mangerite-charnockite pluton of Umarizal, North-east Brazil, *Precambrian Res.*, 87, 19–32, 1998.
- Black, R., L. Latouche, J. P. Liégeois, R. Caby, and J. M. Bertrand, Pan-African displaced terranes in the Tuareg shield (central Sahara), *Geology*, 22, 641–644, 1994.
- Borradale, G. J., and B. Henry, Tectonic applications of magnetic susceptibility and its anisotropy, *Earth Sci. Rev.*, 42, 46–93, 1997.
- Bouchez, J. L., Granite is never isotropic: an introduction to AMS studies of granitic rocks, in *Granite: From Segregation of Melt to Emplacement Fabrics*, edited by J. L. Bouchez, D. H. W. Hutton, and W. E. Evans, pp. 95–112, Kluwer Acad., Norwell, Mass., 1997.
- Brito Neves, B. B., W. R. Van Schmus, E. J. Santos, M. C. Campos Neto, and M. Kozuch, O evento Cariris Velhos na Província Borborema: integração de dados, implicações e perspectivas, *Rev. Bras. Geociênc.*, 25, 279–296, 1995.
- Caby, R., Precambrian terranes of Benin-Nigeria and northeast Brazil and the Late Proterozoic south Atlantic fit, *Spec. Pap. Geol. Soc. Am.*, 230, 145–158, 1989.
- Caby, R., M. Arthaud, and C. J. Archanjo, Lithostratigraphy and petrostructural characterization of supracrustal units in the Brasiliano Belt of Northeast Brazil: Geodynamic implications, *J. S. Am. Earth Sci.*, 8, 235–246, 1995.
- Corsini, M., A. Vauchez, C. J. Archanjo, and E. F. Jardim de Sá, Strain transfer at continental scale from a transcurrent shear zone to a transpressional fold belt: The Patos-Seridó system, northeastern Brazil, *Geology*, 19, 586–589, 1991.
- Corsini, M., L. L. Figueiredo, R. Caby, G. Féraud, G. Ruffet, and A. Vauchez, Thermal history of the Pan-African/Brasiliano Borborema Province of northeast Brazil deduced from  $^{40}\text{Ar}/^{39}\text{Ar}$  analysis, *Tectonophysics*, 285, 103–117, 1998.
- Cosgrove, J. W., The influence of mechanical anisotropy on the behavior of the lower crust, *Tectonophysics*, 280, 1–14, 1997.
- Dantas, E. L., P. C. Hackspacher, W. R. Van Schmus, and B. B. Brito Neves, Archean accretion in the São José do Campestre massif, Borborema Province, northeast Brazil, *Rev. Bras. Geociênc.*, 28, 221–228, 1998.
- Davidson, C., C. Rosenberg, and S. M. Schmid, Syn-magmatic folding of the base of the Bergell pluton, central Alps, *Tectonophysics*, 265, 213–238, 1996.
- Ferré, E., G. Gleizes, and J. L. Bouchez, Internal fabric and strike-slip emplacement of the Pan-African granite of Solli Hills, northern Nigeria, *Tectonics*, 14, 1205–1219, 1995.
- Galindo, A. C., R. Dall'Agnol, I. McReath, J. M. Lafon, and N. Teixeira, Evolution of Brasiliano-age granitoid types in a shear-zone environment, Umarizal-Caraúbas Region, Rio Grande do Norte, northeast Brazil, *J. S. Am. Earth Sci.*, 8, 79–95, 1995.
- Gleizes, G., D. Leblanc, and J. L. Bouchez, Variscan granites on the Pyrenees revisited: Their role as syntectonic markers of the orogen, *Terra Nova*, 9, 38–41, 1997.
- Grégoire, V., J. Darrozes, P. Gaillot, A. Nédélec, and P. Launeau, Magnetite grain shape fabric and distribution anisotropy vs. rock magnetic fabric: A three-dimensional case study, *J. Struct. Geol.*, 20, 937–944, 1998.
- Hackspacher, P. C., and J. M. Legrand, Microstructural and metamorphic evolution of the Portalegre shear zone, northeastern Brazil, *Rev. Bras. Geociênc.*, 19, 63–75, 1986.
- Hackspacher, P. C., E. L. Dantas, B. B. Brito Neves, and J. M. Legrand, Northwestern overthrusting and related lateral escape during the Brasiliano orogeny north of the Patos Lineament, Borborema Province, northeast Brazil, *Int. Geol. Rev.*, 39, 609–620, 1997.
- Hutton, D. H. W., Granite emplacement mechanisms and the tectonic controls: Inferences from deformation studies, *Trans. R. Soc. Edinburgh Earth Sci.*, 79, 245–255, 1988.
- Jardim de Sá, E. F., R. A. Fuck, M. H. F. Macedo, J. J. Peucat, K. Kawashita, Z. S. Souza, and J. M. Bertrand, Pre-Brasiliano orogenic evolution in the Seridó belt, NE Brazil: Conflicting geochronological and structural data, *Rev. Bras. Geociênc.*, 25, 307–314, 1995.
- Jardim de Sá, E. F., R. I. F. Trindade, M. H. B. M. Hollanda, J. M. M. Araújo, A. C. Galindo, V. E. Amaro, Z. S. Souza, J. L. Vignerresse, and J. M. Lardeaux, Brasiliano syntectonic alkaline granites emplaced in a strike-slip/extensional setting (eastern Seridó belt, NE Brazil), *An. Acad. Bras. Ciênc.*, 71, 17–27, 1999.
- Johannes, W., and F. Holtz, *Petrogenesis and Experimental Petrology of Granitic Rocks*, 335 pp., Springer-Verlag, New York, 1996.
- Launeau, P., and A. R. Cruden, Magmatic acquisition mechanisms in a syenite: Results of a combined anisotropy of magnetic susceptibility and image analysis study, *J. Geophys. Res.*, 103, 5067–5089, 1998.
- Leterrier, J., E. F. Jardim de Sá, J. M. Bertrand, and C. Pin, Ages U-Pb sur zircon de granitoides “brasilianos” de la ceinture du Seridó (Province Borborema, NE Brésil), *C. R. Acad. Sci., Sér. II*, 318, 1505–1511, 1994.
- Lima, E. S., Metamorphic conditions in the Seridó region of northeastern Brazil during the Brasiliano Cycle (Late Proterozoic), *J. S. Am. Earth Sci.*, 5, 265–273, 1992.
- Mariano, G., and A. N. Sial, Coexistence and mixing of magmas in the Late Precambrian Itaporanga Batholith, State of Paraíba, northeastern Brazil, *Rev. Bras. Geociênc.*, 20, 101–110, 1990.
- Matos, R. M. D., The northeast Brazilian rift system, *Tectonics*, 11, 766–791, 1992.
- Neves, S. P., and G. Mariano, High-K calc-alkalic plutons in northeast Brazil: Origin of the biotite diorite/quartz monzonite to granite association and implications for the evolution of the Borborema Province, *Int. Geol. Rev.*, 39, 621–638, 1997.
- Paterson, S. R. F. T. K., Jr., K. L. Schmidt, A. S. Yoshinobu, E. S. Yuan, and R. B. Miller, Interpreting magmatic fabric patterns in plutons, *Lithos*, 44, 53–82, 1998.
- Robin, P.-Y. F., and A. R. Cruden, Strain and vorticity patterns in ideally ductile transpression zones, *J. Struct. Geol.*, 16, 447–466, 1994.
- Rochette, P., Magnetic susceptibility of the rock matrix related to magnetic fabric studies, *J. Struct. Geol.*, 9, 1015–1020, 1987.
- Schofield, D. I., and R. S. D'Lemos, Relationships between syn-tectonic granite fabrics and regional PTdt paths: An example from Gander-Avalon boundary of NE Newfoundland, *J. Struct. Geol.*, 20, 459–471, 1998.
- Sial, A. N., A. J. Toselli, J. Saavedra, M. A. Parada, and V. P. Ferreira, Emplacement, petrological and magnetic susceptibility characteristics of diverse magmatic epidote-bearing granitoid rocks in Brazil, Argentina and Chile, *Lithos*, 46, 367–392, 1999.
- Souza, Z. S., H. Martin, M. H. F. Macedo, J. J. Peucat, and E. F. Jardim de Sá, Un segment de croûte continentale juvénile d'âge protérozoïque inférieur: Le complexe de Caicó (Rio Grande do Norte, NE-Brésil), *C. R. Acad. Sci., Sér. II*, 316, 201–208, 1993.
- Tommasi, A., and A. Vauchez, Continental-scale rheological heterogeneities and complex intraplate tectono-metamorphic patterns: Insights from a case-study and numerical models, *Tectonophysics*, 279, 327–350, 1997.
- Trindade, R. I. F., Magnetismo de corpos graníticos e a evolução tectônica brasileira da porção ocidental da Faixa Seridó (NE do Brasil), Ph.D. thesis, 184 pp., Univ. de São Paulo, Brazil, 1999.
- Trindade, R. I. F., M. I. B. Raposo, M. Ernesto, and R. Siqueira, Magnetic susceptibility and partial anhysteretic remanence anisotropies in the magnetite-bearing granite pluton of Tourão, NE Brazil, *Tectonophysics*, 314, 443–468, 1999.
- Unrug, R., Geodynamic Map of the Gondwana Supercontinent Assembly, in *IGCP Project 288, Gondwana Sutures and Fold Belts*, Council for Geosci., Pretoria, South Africa and Bur. de Rech. Géol. et Minières, Orleans, France, 1996.
- Van Schmus, W. R., B. B. Brito Neves, P. C. Hackspacher, and M. Babinski, U/Pb and Sm/Nd geochronologic studies of the eastern Borborema Province, northeastern Brazil: Initial conclusions, *J. S. Am. Earth Sci.*, 8, 267–288, 1995.
- Vauchez, A., S. P. Neves, R. Caby, M. Corsini, M. Egydio-Silva, M. Arthaud, and V. E. Amaro, The Borborema shear zone system, NE Brazil, *J. S. Am. Earth Sci.*, 8, 247–266, 1995.
- Vignerresse, J. L., and B. Tikoff, Strain partitioning during partial melting and crystallizing felsic magmas, *Tectonophysics*, 312, 117–132, 1999.
- Wiebe, R. A., and W. J. Collins, Depositional features and stratigraphic sections in granite plutons: Implications for the emplacement and crystallization of granitic magma, *J. Struct. Geol.*, 20, 1273–1289, 1998.

C. J. Archanjo, Instituto de Geociências/GMG, Universidade de São Paulo, rua do Lago 562, São Paulo, SP, 05508-900 Brasil. (archan@usp.br)

J. L. Bouchez, Unité Mixte de Recherche, 1563 Mécanismes de Transfert en Géologie, Observatoire Midi-Pyrénées-Université Paul-Sabatier, 38 rue des Trente-Six Ponts, Toulouse, F-31400 France. (bouchez@lucid.univ-tlse.fr)

M. Ernesto and R. I. F. Trindade, Instituto Astronômico e Geofísico, Universidade de São Paulo, rua do Matão 1226, São Paulo, SP, 05508-900 Brasil. (marcia@iag.usp.br; rtrindad@yahoo.com.br)